Published in final edited form as:

Nat Biotechnol. 2017 March ; 35(3): 280–284. doi:10.1038/nbt.3781.

A synthetic AAV vector enables safe and efficient gene transfer to the mammalian inner ear

Lukas D. Landegger[1,2,3,*], **Bifeng Pan**[2,4,*], **Charles Askew**[2,4,*,'], **Sarah Wassmer**[5,6], **Sarah Gluck**[2,4,7], **Alice Galvin**[4], **Ruth Taylor**[8], **Andrew Forge**[8], **Konstantina M. Stankovic**[1,2,7,#], **Jeffrey R. Holt**[2,4,9,#], and **Luk H. Vandenberghe**[5,6,10,#]

[1]Eaton Peabody Laboratories, Department of Otolaryngology, Massachusetts Eye and Ear, Boston, Massachusetts, USA

[2]Department of Otolaryngology, Harvard Medical School, Boston, Massachusetts, USA

[3]Department of Otolaryngology, Vienna General Hospital, Medical University of Vienna, Vienna, Austria

[4]Department of Otolaryngology, F.M. Kirby Neurobiology Center, Boston Children's Hospital, Boston, Massachusetts, USA

[5]Grousbeck Gene Therapy Center, Schepens Eye Research Institute and Massachusetts Eye and Ear, Boston, Massachusetts, USA

[6]Ocular Genomics Institute, Department of Ophthalmology, Harvard Medical School, Boston, Massachusetts, USA

[7]Harvard Program in Speech and Hearing Bioscience and Technology, Boston, MA, USA

[8]Center for Auditory Research, UCL Ear Institute, London, UK

[9]Department of Neurology, Boston Children's Hospital and Harvard Medical School, Boston, Massachusetts, USA

[10]Harvard Stem Cell Institute, Harvard University, Cambridge, Massachusetts, USA

Correspondence should be addressed to L.H.V. (luk_vandenberghe@meei.harvard.edu) at Massachusetts Eye and Ear, Boston, Massachusetts 02114, USA), J.R.H. (jeffrey.holt@childrens.harvard.edu) at Boston Children's Hospital, Boston, Massachusetts 02115, USA, or K.M.S. (konstantina_stankovic@meei.harvard.edu) at Massachusetts Eye and Ear, 243 Charles St. Boston, Massachusetts 02114, USA.

[']Present address: Gene Therapy Center, University of North Carolina at Chapel Hill, Chapel Hill, North Carolina, USA

[*, #]These authors contributed equally to this work (done in Boston, MA, USA).

Accession Codes and Data availability Statement

Anc80L65 sequences are available at GenBank Accession number AKU89595[3].

Author Contributions

L.D.L., B.P, C.A., S.W., S.G., A.G. conducted the gene transfer experiments described, R.T., A.F. performed and led the human vestibular transduction experiments. L.H.V. provided vector materials. L.D.L., K.M.S, J.R.H. and L.H.V. designed and reported the experiments with topical input from all other authors.

Competing Financial Interests

L.H.V. holds founder equity in GenSight Biologics, is a consultant to a number of biotech and pharmaceutical companies, and is an inventor on gene therapy patents, including Anc80L65 which are licensed to various entities. L.H.V also receives sponsored research from Lonza Houston and Selecta Biosciences, licensees of Anc80L65. L.H.V., K.M.S. and J.R.H. have filed a patent on the use of Anc80L65 in the cochlea.

Abstract

Efforts to develop gene therapies for hearing loss have been hampered by the lack of safe, efficient, and clinically relevant delivery modalities[1, 2]. Here we demonstrate the safety and efficiency of Anc80L65, a rationally designed synthetic vector[3], for transgene delivery to the mouse cochlea. Cochlear explants incubated with Anc80L65 encoding eGFP demonstrated high level transduction of inner and outer hair cells (60–100%). Injection of Anc80L65 through the round window membrane resulted in highly efficient transduction of inner and outer hair cells, a substantial improvement over conventional adeno-associated virus (AAV) vectors. Anc80L65 round window injection was well tolerated, as indicated by sensory cell function, hearing and vestibular function, and immunologic parameters. The ability of Anc80L65 to target outer hair cells at high rates, a requirement for restoration of complex auditory function, may enable future gene therapies for hearing and balance disorders.

Hearing loss is the most common sensory disorder worldwide, with half of pre-lingual deafness due to genetic causes[4]. More than 300 genetic loci linked to hereditary hearing loss and >100 causative genes have also been identified[4, 5]. Age-related hearing impairment affects the quality of life of over a quarter of individuals over 65 years old. While medication history and noise exposure are known contributing factors to presbycusis, several genetic factors have been identified[6]. Sensory cells of the adult mammalian cochlea lack the capacity for self-renewal[7, 8]. Current therapies for hearing loss employ various strategies depending on the level and exact position of impairment, including sound amplification (hearing aids), enhanced sound transmission (middle ear prostheses/active implants), and direct neuronal stimulation (cochlear implants) to compensate for permanent damage to primary sensory hair cells or to spiral ganglion neurons, which form the auditory nerve and relay acoustic information to the brain[2]. These approaches, while transformative, remain far from optimal in restoring complex hearing function and may have deficiencies in frequency sensitivity, natural sound perception, and speech discrimination in noisy environments.

Therapeutic gene transfer to the cochlea could improve on the current standard of care for both genetic[1, 2, 9–13] and age-related or environmentally induced hearing loss[1, 2, 12, 13]. This approach would require the development of methods for safe, efficient delivery of transgene constructs to the relevant cell types in the organ of Corti in the cochlea. The organ of Corti includes two classes of sensory hair cells: inner hair cells (IHCs), which convert mechanical information carried by sound into electrical signals transmitted to neuronal structures, and outer hair cells (OHCs), which amplify and tune the cochlear response, a process required for complex hearing function[14]. Other potential targets in the inner ear include spiral ganglion neurons, columnar cells of the spiral limbus, which are important for the maintenance of the adjacent tectorial membrane[15–17], and supporting cells, which have protective functions and can be triggered to transdifferentiate into hair cells up to an early neonatal stage[18–21].

Direct access to hair cells for gene therapy may be achievable through vector injection into the cochlear duct. However, interventions that alter the delicate high-potassium endolymph fluid in the duct could disrupt the endocochlear potential, leading to damage of the sensory cells and irreversible hearing loss. The perilymph-filled spaces surrounding the cochlear

duct, scala tympani and scala vestibuli can be accessed from the middle ear, either through the oval window membrane or the round window membrane (RWM). The RWM, which is the only non-bony opening into the inner ear, is relatively easily accessible in many animal models, and administration of viral vector using this route has been well tolerated[10, 11, 22]. In humans, cochlear implant placement routinely relies on surgical electrode insertion through the RWM[23].

Several non-viral[24, 25] and viral (e.g., adenovirus, AAV, lentivirus, herpes simplex virus I, vaccinia virus) gene transfer vectors have been tested in the cochlea often with only transient or suboptimal gene transfer as a result[1]. Only adenovirus to date has progressed to a clinical program (NCT02132130)[2, 26]. For other target organs, such as the liver and the retina, AAV has shown clinical efficacy and safety in hemophilia B[27], two types of inherited blindness[28, 29], and familial lipoprotein lipase deficiency[30]. Previous studies of AAV serotypes *in vivo* inner ear injection via different routes of administration highlighted the difficulties in targeting OHCs, particularly via RWM injection[31], and resulted in only partial rescue of hearing in mouse models of inherited deafness[9–11]. To identify vectors that target both IHCs and OHCs with high efficiency, we evaluated natural AAVs, alongside a recently developed synthetic AAV called Anc80L65. The latter *in silico* designed particle approximates the ancestral state of the viral capsid within the lineage of the commonly used AAV serotypes 1, 2, 6, 8, and 9 and is a structurally stable and antigenically distinct AAV[3]. Importantly, Anc80L65 was shown to be a potent gene transfer agent in liver, retina, and muscle, which led us to characterize its tropism in the inner ear *in vivo*.

Results

In a first selection, we incubated iodixanol-purified high-titer preparations of single-stranded AAV1, 2, 6, 8, 9, and Anc80L65 encoding eGFP driven from the cytomegalovirus immediate-early (CMV) promoter, at equal doses of 10^{10} genome-containing (GC) particles, with organotypic cochlear explants from C57BL/6 or CBA/CaJ mice harvested at postnatal day (P) P4. We performed histology of the inoculated cochleas after 2 days of vector exposure. The results in Fig. 1 and Supplementary Fig. 1 illustrate the tropism of the five conventional AAV serotypes and Anc80L65 as monitored by eGFP expression in C57BL/6 and CBA/CaJ, respectively. eGFP expression was qualitatively brighter in cochlear cultures exposed to Anc80L65, with expression apparent in many cochlear cell types (Fig. 1 and Supplementary Fig. 1). Morphometric quantitative analysis was performed to determine transduction rates for IHCs, OHCs, supporting cells, limbus cells, and spiral ganglion neurons. For IHCs and OHCs, vector transduction efficiency was quantified as the percentage of eGFP-positive cells in representative 100 micron sections taken from the basal and apical regions of the cochlea. Anc80L65 targeted IHCs and OHCs at efficiencies between 60 and 100% in apical and basal regions of both mouse strains tested (Fig. 1H, I and Supplementary Fig. 1G, H). Anc80L65 demonstrated consistently and qualitatively brighter IHC and OHC eGFP expression as compared to AAV2 (Fig. 1 and Supplementary Fig. 1).

To control for possible differences between the AAV serotypes in the onset of transgene expression, which could lead to an underestimate of expression at the 2-day time point, we

repeated the above experiment with a new set of cochleas and maintained the culture for an additional 5 days (referred to as 48h+5d). A similar pattern of expression in IHCs and OHCs was observed in this longer-term study for AAV2 and Anc80L65 (Fig. 1J, K and Supplementary Fig. 1I, J). Moderate increases in expression for AAV6, 8, and 9 in CBA/CaJ mice, particularly at the basal turn (Fig. 1J, K, and Supplementary Fig. 1I, J), were noted. Other cell types were targeted by all serotypes, with limbus being more permissive than supporting cells, followed by spinal ganglion neurons (Supplementary Fig. 2, 3, and 4). Consistently, Anc80L65 transduction yielded higher efficiencies and stronger expression, evidenced by brighter eGFP fluorescence (Fig. 1 and Supplementary Fig. 1–4).

Next, we evaluated the tropism and gene transfer efficiency of AAV1, 2, 6, 8, and Anc80L65 *in vivo*, using a protocol that is therapeutically relevant with respect to vector pharmacokinetics, anatomical and cellular barriers to transduction, and surgical approach. C57BL/6 animals were injected at P1 and cochleas were harvested, fixed and stained at P10. Consistent with prior reports[9–11, 32], AAV1 transduced IHCs with moderate to high efficiency (Fig. 2A, B). Our results indicated that AAV2, 6, and 8 target low numbers of IHCs (Fig. 2A, B). Also, consistent with prior reports, transduction of OHCs was minimal (<5%) for all conventional AAV serotypes tested. In contrast, Anc80L65 transduced nearly 100% of IHCs and ~90% of OHCs (Fig. 2A–C) at a 20- (for AAV1) to 3-fold (for AAV2) lower dose. Transduction at equal dose of 1.36×10^{12} GC for all serotypes resulted in substantial IHC and OHC transduction for Anc80L65, but minimal IHC targeting for AAV1, 2, and 8, and none noted in OHCs as observed by live-cell imaging by epifluorescence microscopy (Fig. 3C, D).

The Anc80L65-transduced samples were subsequently fixed, stained and imaged, revealing a dose-dependence of hair cell transduction (Fig. 3E). The unprecedented high level of OHC targeting (Fig. 2C, Fig. 3) suggests that the transduction mechanism of Anc80L65 is qualitatively different from that of other AAVs. We found similar levels of Anc80L65 transduction throughout the cochlea from base to apex in a total of three Anc80L65-injected mice (Fig. 2A, B, C). Low-magnification views of the cochlear apex (Fig. 3A) show strong eGFP expression far from the injection site. High-magnification images of the base reveal 100% IHC and 95% OHC transduction (Fig. 3B).

In some animals, we found robust eGFP expression in the contralateral uninjected ear (Supplementary Fig. 5). In mice, the cochlear aqueduct is patent, providing a fluid path from the cochlear perilymph into the cerebrospinal fluid, the contralateral aqueduct and into the contralateral cochlea. We therefore investigated whether Anc80L65-eGFP injected via the RWM transduced neurons in the brain. Cross-sections of the cerebellum revealed strong eGFP expression in cerebellar Purkinje neurons (Supplementary Fig. 6A, B).

We further investigated whether Anc80L65 RWM injection led to a humoral response to the vector capsid and found that low neutralization to vector was detectable in injected mice in serum, but not in cerebrospinal fluid, at the level of sensitivity of the assay and sampling (Supplementary Fig. 6C).

To determine whether Anc80L65-eGFP had any consequences for cellular function, we recorded sensory transduction currents from both IHCs and OHCs. Representative currents evoked by hair bundle deflections from P7 OHCs and P35 IHCs revealed no differences in amplitude, sensitivity or kinetics, between eGFP-positive and eGFP-negative control cells (Fig. 2D). We recorded from 51 eGFP-positive and 52 eGFP-negative hair cells from all regions of the cochlea and ages between one and five weeks after exposure to Anc80L65. Responses were indistinguishable from wild-type in all cases (Fig. 2E), which confirmed that Anc80L65 transduction had no detrimental effects on sensory cell function.

To evaluate systems level function, we measured auditory brainstem responses (ABRs) from four Anc80L65-injected ears and four uninjected ears. Minimal sound thresholds required to evoke ABRs were plotted (Fig. 2F) and revealed no difference in threshold between injected and uninjected ears. Histological analysis showed strong eGFP fluorescence in all four injected ears (data not shown). In one additional case, there were no eGFP-positive cells and ABR thresholds were elevated (Fig. 2F), suggesting that the injection failed and that the needle may have breached the cochlear duct and caused permanent damage.

As a final test of auditory function, we measured distortion product otoacoustic emissions (DPOAEs), which is an assay for proper cochlear amplification and tuning and is a sensitive measure of OHC viability[17]. Despite robust OHC transduction by Anc80L65-eGFP, we found no difference in DPOAE thresholds relative to uninjected control ears (Fig. 2G). Thus, data from all three measures---single cell physiology, ABRs, and DPOAEs---indicate that RWM injection, Anc80L65 transduction and eGFP expression in IHCs and OHCs are safe and do not harm auditory function.

Since the perilymphatic solutions of the cochlea are continuous with those of the vestibular labyrinth, we wondered whether Anc80L65-eGFP injected via the cochlear RWM would transduce vestibular sensory organs. Indeed, whole-mounts of vestibular epithelia revealed robust eGFP expression in both type I and type II hair cells of the utricle, a vestibular organ sensitive to gravity and linear head movements and in the semicircular canals, which are sensitive to rotational head movements (Fig. 4A, B). To address the safety concern that Anc80L65 transduction may affect balance, we used the rotarod test for vestibular function. Injected mice performed similarly to uninjected controls (P = 1.00, Supplementary Fig. 7).

Some forms of genetic deafness also cause vestibular dysfunction, and Anc80L65 may be a useful vector for gene delivery into human vestibular organs. To investigate this possibility, we harvested human vestibular epithelia from four adult patients undergoing resection of vestibular schwannoma tumors and placed the sensory epithelium in culture as previously described[33]. Figure 4C reveal for AAV-transduced samples strong eGFP fluorescence throughout the human vestibular epithelium in both hair cells and supporting cells. A high-magnification view in an epithelium counterstained with Myo7A in Figure 4D revealed that 83% (19/23) of Myo7A-positive hair cells were also eGFP-positive, suggesting that Anc80L65 can transduce both mouse and human hair cells efficiently.

Discussion

Our finding that Anc80L65 transduces OHCs with high efficiency overcomes the low transduction rates that have limited development of cochlear gene therapy using conventional AAV serotypes. Thus, Anc80L65 may provide a valuable approach for gene delivery to human IHCs *and* OHCs, as well as to other inner ear cell types that are compromised by genetic hearing and balance disorders. Previous work has shown that Anc80L65 has an analogous safety profile in mouse and nonhuman primate after systemic injection, and is antigenically distinct from circulating AAVs, providing a potential benefit in terms of pre-existing immunity, which limits the efficacy of conventional AAV vectors[4].

Further validation of Anc80L65 as a gene transfer vector for use in human inner ear gene therapy will require targeting efficiency studies in large-animal models; additional exploration of the window of opportunity for therapeutic intervention; and pharmacology and toxicology studies to investigate the safety of Anc80L65 upon cochlear administration. Given the promiscuity of expression of AAV, including Anc80L65, additional methods to maximize specificity and minimize biodistribution should be considered to limit expression outside of the therapeutic cochlear cell target. Considering that nonsyndromic auditory and vestibular dysfunction can be caused by dominant or recessive mutations in >100 genes, Anc80L65 may accelerate the development of novel gene therapy strategies for a wide range of inner ear disorders.

Online Methods

Animal models and general methods

All experiments were approved by the respective Institutional Animal Care and Use Committees at Massachusetts Eye and Ear (protocol #15-003) and Boston Children's Hospital (protocol #12-02-2146) as well as the Institutional Biosafety Committee (protocol #IBC-P00000447). Wild-type C57BL/6J and CBA/CaJ mice were obtained from the Jackson Laboratory (Bar Harbor, ME) and animals of either sex were used for experimentation in an estimated 50/50 ratio. Group sizes per experiment for the *in vitro* and *in vivo* transduction assays and subsequent endpoints were determined by access to specimen and technical feasibility. Reported observations on Anc80L65 transduction were qualitatively validated in subsequent experiments with various vector lots (except for the human vestibular tissue transduction due to the unique and limited nature of access to specimen). No statistical analysis between serotype transduction efficiencies was performed due to the limited access to specimen and qualitative nature of the reported findings.

Viral vectors

AAV2/1, 2/2, 2/6, 2/8, 2/9, and AAV2/Anc80L65 with a CMV-driven eGFP transgene and the Woodchuck hepatitis virus Post-transcriptional Regulatory Element (WPRE) cassette were prepared at Gene Transfer Vector Core (vector.meei.harvard.edu) at Massachusetts Eye and Ear as previously described[3]. AAV2/Anc80L65 plasmid reagents are available through addgene.com.

In vitro explant cultures

A total of 156 cochlear explant cultures from mouse pups of both strains were prepared on postnatal day 4[34]. In brief, murine temporal bones were harvested after decapitation and the cochlea was dissected to culture as organotypic explants connected to the spiral ganglion neuron region. Two specimens were obtained per cochlea, one ("apical") consisting of the lower apical and one ("basal") of the upper basal turn. For each serotype, a minimum of 3 (CBA/CaJ, 48h), 2 (CBA/CaJ, 48h+5d), 3 (C57BL/6, 48h), 2 (C57BL/6, 48h+5d) basal and apical specimens were inoculated. Specimens were excluded if cochlear morphology was not retained during the culture. Sample numbers were chosen to inform on the variability of transduction and to provide a basis for selection for further *in vivo* evaluation. Explants were incubated with culture medium (98% Dulbecco's Modified Eagle Medium (DMEM), 1% ampicillin, and 1% N2 supplement during the first 12 hours, plus 1% fetal bovine serum (FBS)) and 10^{10} GC of AAV for 48h in 50 μl. For the 48h+5d condition, the medium with AAV was replaced with fresh media without AAV for an additional 5 days.

Human vestibular epithelia from utricles obtained from four consented, adult patients undergoing vestibular schwannoma tumor resection were cultured as previously described[33], exposed to 10^{10} GC AAV for 24 hours and maintained in culture for 10 days after which the tissue was fixed and stained with phalloidin and imaged. Studies were approved by the Surrey Borders NRES Committee London (Health Research Authority) under reference number 11/LO/0475.

In vivo injections

Mouse pups (P0 to P2) were injected via the round window membrane (RWM) using beveled glass microinjection pipettes. Pipettes were pulled from capillary glass (WPI, Sarasota, FL) on a P-2000 pipette puller (Sutter Instrument, Novato, CA) and were beveled (~20 μm tip diameter at a 28° angle) using a micropipette beveler (Sutter Instrument, Novato, CA). EMLA cream (lidocaine 2.5% and prilocaine 2.5%) was applied externally for analgesia using sterile swabs to cover the surgical site (left mastoid prominence). Body temperature was maintained on a 38 °C warming pad prior to surgery. Pups were anesthetized by rapid induction of hypothermia into ice/water for 2–3 minutes until loss of consciousness, and this state was maintained on a cooling platform for 5–10 minutes during the surgery. The surgical site was disinfected by scrubbing with Betadine and wiping with 70% Ethanol in repetition three times. A post-auricular incision was made to expose the transparent otic bulla, a micropipette was advanced manually through the bulla and overlying fascia, and the RWM was penetrated by the tip of the micropipette. Approximately 1 μL of virus at the available concentration was injected unilaterally within 1 min into the left ear manually in 5 (AAV1), 4 (AAV2), 2 (AAV8), 1 (AAV6), 3 (Anc80L65) C57BL/6 animals and quantification was performed on a representative specimen per vector. In order to control for factors related to the specific vector preparation such as quality and purity, Anc80L65 results were confirmed in subsequent studies with different vector lots from independent preparation which were confirmatory of our qualitative findings presented here (data not shown). Injections were performed per group in a non-blinded fashion. Occasionally, the injection needle was inserted too deep, too shallow or at the wrong angle. If there was visible damage to the middle or inner ear structures, the samples were excluded

from further analysis. Success rates of injection ranged between ~50% to ~80% depending on the experience level of the injector. After the injection, the skin incision was closed using a 6-0 black monofilament suture (Surgical Specialties, Wyomissing, PA). Pups were subsequently returned to the 38 °C warming pad for 5–10 min and then put back to their mother for breeding.

Hearing tests

Auditory brainstem response (ABR) and distortion product otoacoustic emissions (DPOAE) data were collected as described previously[10]. Stimuli tested in anesthetized mice varied between 10 and 90 dB sound pressure level at frequencies of 5.6, 8, 11.3, 16, 22.6, and 32 kHz. Four Anc80L65-injected ears, four uninjected ears, and one negative control ear with injection damage without eGFP fluorescence were analyzed at P28-P30.

Cerebrospinal fluid and blood sampling

Cerebrospinal fluid (CSF) sampling from the cisterna magna[35] and intracardiac blood collection with thoracotomy were performed in a terminal procedure. Through the microcapillary tube, the maximum amount (up to 5 μL) of clear CSF per animal was collected in a volume of 60 μL PBS, leading to slightly different starting dilutions that subsequently were standardized with additional control PBS prior to the start of the experiment. After obtaining the blood sample in a 1.1 mL Z-Gel micro tube (Sarstedt, Nümbrecht, Germany), it was spun down at 8,000 rpm for 8 minutes and serum was stored together with the CSF sample (in PBS) at −80 °C until further use.

Histological analysis

After a follow-up period of 5 to 29 days, animals were sacrificed and cochlear whole-mounts were prepared as previously reported[36]. Both cochlear whole-mounts and explants were stained with antibodies against myosin 7A (Myo7A, #25-6790 Proteus Biosciences, Ramona, CA, 1:400) and β-tubulin (TuJ1, #MMS-435P Biolegend, San Diego, CA, 1:200), together with corresponding secondary antibodies (Alexa Fluor 555 anti-mouse and Alexa Fluor 647 anti-rabbit, #A-21422 and #A-21245 Thermo Fisher Scientific, Waltham, MA, 1:1000)[34]. Mounting of the specimens was followed by confocal microscopy. Every image of a given experimental series was obtained with the same settings, with laser intensity being chosen based on the specimen with the strongest eGFP signal to prevent fluorescence saturation. Z-stacks for overview images and zoomed-in pictures for the organ of Corti and spiral ganglion neuron areas were obtained. 3D reconstruction with AMIRA was used to determine spiral ganglion neuron transfection more accurately.

Quantification of eGFP-expression

For *in vitro* data, the percentage of eGFP-positive inner (IHCs) and OHCs (OHCs) was manually quantified along the cochlea, by dividing the number of eGFP-positive cells by the total number of outer or inner hair cells per one or two 100 μm sections per basal and apical sample for each specimen. All visible spiral ganglion neurons in a cochlear explant were evaluated regarding their eGFP expression. The areas of the spiral limbus and supporting cells were assessed with a qualitative approach (as explained above, adjusted for each

experimental series) by means of a scale from 0 (no expression) to 3 (strongest signal). Control samples without AAV were used to exclude autofluorescence.

Immunological assays

Antibody titers against Anc80L65 in CSF and serum were determined through neutralization assays[3]. Using a 96-well format, heat-inactivated CSF or serum samples (collected as described above) were serially diluted in serum-free medium (Life Technologies, Carlsbad, CA), and then treated with Anc80L65-luciferase (10^6 GC/well) for 1 hour at 37 °C. The sample/Anc80L65-luciferase mix was then transferred onto HEK293 cells, which were treated with adenovirus (MOI 20) the day before. After 1 hour at 37 °C, diluted serum medium (1 part serum-free, 2 parts with serum) was added to each well. Two days later, the cells were treated with lysis buffer (Promega, Madison, WI) and frozen at −80 °C for 30 minutes. The cells were then thawed at 37 °C for 15 minutes before being treated with substrate buffer (Tris-HCl, $MgCl_2$, ATP [Life Technologies, Carlsbad, CA], D-Luciferin [Caliper Life Sciences, Hopkinton, MA]). Luminescence output was read using the Synergy BioTek Plate Reader (BioTek, Winooski, VT).

Hair cell electrophysiology

Cochleas were excised, mounted on glass coverslips and viewed on an Axio Examiner.A1 upright microscope (Carl Zeiss, Oberkochen, Germany) equipped with a 63x water-immersion objective and differential interference contrast optics. Electrophysiological recordings were performed at room temperature (22 °C–24 °C) in standard solutions containing (in mM): 137 NaCl, 5.8 KCl, 10 HEPES, 0.7 NaH_2PO_4, 1.3 $CaCl_2$, 0.9 $MgCl_2$, and 5.6 D-glucose, vitamins (1:100), and amino acids (1:50) as in MEM (Life Technologies, Carlsbad, CA) (pH 7.4; ~310 mOsm/kg). Recording electrodes (3–4 MΩ) were pulled from R-6 glass (King Precision Glass, Claremont, CA) and filled with intracellular solution containing (in mM): 140 CsCl, 5 EGTA-KOH, 5 HEPES, 2.5 Na_2ATP, 3.5 $MgCl_2$, and 0.1 $CaCl_2$ (pH 7.4; ~280 mOsm/kg). The whole-cell, tight-seal technique was used to record mechanotransduction currents using an Axopatch 200B (Molecular Devices, Sunnyvale, CA). Hair cells were held at −84 mV. Currents were filtered at 5 kHz with a low-pass Bessel filter, digitized at ≥20 kHz with a 12-bit acquisition board (Digidata 1440A, Molecular Devices, Sunnyvale, CA), and recorded using pCLAMP 10 software (Molecular Devices, Sunnyvale, CA). Hair bundles from IHCs and OHCs were deflected using stiff glass probes mounted on a PICMA chip piezo actuator (Physik Instrumente, Karlsruhe, Germany) driven by an LVPZT amplifier (E-500.00, Physik Instrumente, Karlsruhe, Germany) and filtered with an 8-pole Bessel filter (Model 3384 filter, Krohn-Hite Corporation, Brockton, MA) at 40 kHz to eliminate residual pipette resonance. Stiff glass probes were designed to fit into the concave aspect of the array of hair cell stereocilia for whole-bundle recordings (3–4 μm diameter for OHCs and 4–5 μm diameter for IHCs). For the whole-cell electrophysiology recording at >P10, cochlea tissues were dissected at P5-7 and incubated in MEM(1X) + GlutaMAX™-I medium with 1% FBS at 37 °C, 5% CO_2 for up to 30 days.

Statistical tests

Descriptive statistics for *in vitro* and *in vivo* eGFP expression data are presented. Rotarod results were analyzed with a two-tailed t-test. Error bars, n values, and type of replicates for experiments are defined in the respective paragraphs and figure legends.

Supplementary Material

Refer to Web version on PubMed Central for supplementary material.

Acknowledgments

This work was supported by the Bertarelli Foundation grants (KMS, JRH), the Jeff and Kimberly Barber Gene Therapy Research Fund (JRH), the Patel Gene Therapy Fund (JRH), Department of Defense Grant W81XWH-15-1-0472 (KMS), the National Institutes of Health 1R01DC015824 (KMS), Nancy Sayles Day Foundation (KMS), Lauer Tinnitus Research Center (KMS), Grousbeck Family Foundation (LHV), Foundation Fighting Blindness (LHV), Ush2A Consortium (LHV) and NIH 5DP1EY023177 (LHV). The authors would like to thank H.-C. Lin and S. Narasimhan) for help with the brain tissue staining protocol, G. Geleoc and C. Nist-Lund for assistance with vestibular tissue imaging, and R. Xiao, R. Shelke, Y. Lin, and T. Barungi for vector preparation.

References

1. Fukui H, Raphael Y. Gene therapy for the inner ear. Hearing research. 2013; 297:99–105. [PubMed: 23265411]
2. Geleoc GS, Holt JR. Sound strategies for hearing restoration. Science. 2014; 344:1241062. [PubMed: 24812404]
3. Zinn E, et al. In Silico Reconstruction of the Viral Evolutionary Lineage Yields a Potent Gene Therapy Vector. Cell reports. 2015; 12:1056–1068. [PubMed: 26235624]
4. Parker M, Bitner-Glindzicz M. Genetic investigations in childhood deafness. Archives of disease in childhood. 2015; 100:271–278. [PubMed: 25324569]
5. Stamatiou GA, Stankovic KM. A comprehensive network and pathway analysis of human deafness genes. Otology & neurotology : official publication of the American Otological Society, American Neurotology Society [and] European Academy of Otology and Neurotology. 2013; 34:961–970.
6. Hoffmann TJ, et al. A Large Genome-Wide Association Study of Age-Related Hearing Impairment Using Electronic Health Records. PLoS Genet. 2016; 12:e1006371. [PubMed: 27764096]
7. Rubel EW, Furrer SA, Stone JS. A brief history of hair cell regeneration research and speculations on the future. Hearing research. 2013; 297:42–51. [PubMed: 23321648]
8. Groves AK. The challenge of hair cell regeneration. Exp Biol Med (Maywood). 2010; 235:434–446. [PubMed: 20407075]
9. Akil O, et al. Restoration of hearing in the VGLUT3 knockout mouse using virally mediated gene therapy. Neuron. 2012; 75:283–293. [PubMed: 22841313]
10. Askew C, et al. Tmc gene therapy restores auditory function in deaf mice. Science translational medicine. 2015; 7:295ra108.
11. Chien WW, et al. Gene Therapy Restores Hair Cell Stereocilia Morphology in Inner Ears of Deaf Whirler Mice. Mol Ther. 2016; 24:17–25. [PubMed: 26307667]
12. Izumikawa M, et al. Auditory hair cell replacement and hearing improvement by Atoh1 gene therapy in deaf mammals. Nat Med. 2005; 11:271–276. [PubMed: 15711559]
13. Chien WW, Monzack EL, McDougald DS, Cunningham LL. Gene therapy for sensorineural hearing loss. Ear and hearing. 2015; 36:1–7. [PubMed: 25166629]
14. LeMasurier M, Gillespie PG. Hair-cell mechanotransduction and cochlear amplification. Neuron. 2005; 48:403–415. [PubMed: 16269359]
15. Spicer SS, Thomopoulos GN, Schulte BA. Structural evidence for ion transport and tectorial membrane maintenance in the gerbil limbus. Hearing research. 2000; 143:147–161. [PubMed: 10771192]

16. Gavara N, Manoussaki D, Chadwick RS. Auditory mechanics of the tectorial membrane and the cochlear spiral. Current opinion in otolaryngology & head and neck surgery. 2011; 19:382–387. [PubMed: 21785353]
17. Guinan JJ Jr, Salt A, Cheatham MA. Progress in cochlear physiology after Bekesy. Hearing research. 2012; 293:12–20. [PubMed: 22633944]
18. White PM, Doetzlhofer A, Lee YS, Groves AK, Segil N. Mammalian cochlear supporting cells can divide and trans-differentiate into hair cells. Nature. 2006; 441:984–987. [PubMed: 16791196]
19. Bramhall NF, Shi F, Arnold K, Hochedlinger K, Edge AS. Lgr5-positive supporting cells generate new hair cells in the postnatal cochlea. Stem cell reports. 2014; 2:311–322. [PubMed: 24672754]
20. May LA, et al. Inner ear supporting cells protect hair cells by secreting HSP70. The Journal of clinical investigation. 2013; 123:3577–3587. [PubMed: 23863716]
21. Mellado Lagarde MM, et al. Spontaneous regeneration of cochlear supporting cells after neonatal ablation ensures hearing in the adult mouse. Proceedings of the National Academy of Sciences of the United States of America. 2014; 111:16919–16924. [PubMed: 25385613]
22. Chien WW, McDougald DS, Roy S, Fitzgerald TS, Cunningham LL. Cochlear gene transfer mediated by adeno-associated virus: Comparison of two surgical approaches. The Laryngoscope. 2015; 125:2557–2564. [PubMed: 25891801]
23. Nguyen S, et al. Outcomes review of modern hearing preservation technique in cochlear implant. Auris Nasus Larynx. 2016; 43:485–488. [PubMed: 26976547]
24. Zou B, et al. The application of genome editing in studying hearing loss. Hearing research. 2015; 327:102–108. [PubMed: 25987504]
25. Zuris JA, et al. Cationic lipid-mediated delivery of proteins enables efficient protein-based genome editing in vitro and in vivo. Nat Biotechnol. 2015; 33:73–80. [PubMed: 25357182]
26. Luebke AE, Rova C, Von Doersten PG, Poulsen DJ. Adenoviral and AAV-mediated gene transfer to the inner ear: role of serotype, promoter, and viral load on in vivo and in vitro infection efficiencies. Advances in oto-rhino-laryngology. 2009; 66:87–98. [PubMed: 19494574]
27. Nathwani AC, et al. Adenovirus-associated virus vector-mediated gene transfer in hemophilia B. The New England journal of medicine. 2011; 365:2357–2365. [PubMed: 22149959]
28. Maguire AM, et al. Safety and efficacy of gene transfer for Leber's congenital amaurosis. The New England journal of medicine. 2008; 358:2240–2248. [PubMed: 18441370]
29. MacLaren RE, et al. Retinal gene therapy in patients with choroideremia: initial findings from a phase 1/2 clinical trial. Lancet. 2014; 383:1129–1137. [PubMed: 24439297]
30. Bryant LM, et al. Lessons learned from the clinical development and market authorization of Glybera. Human gene therapy Clinical development. 2013; 24:55–64. [PubMed: 23808604]
31. Liu Y, et al. Specific and efficient transduction of Cochlear inner hair cells with recombinant adeno-associated virus type 3 vector. Mol Ther. 2005; 12:725–733. [PubMed: 16169458]
32. Kilpatrick LA, et al. Adeno-associated virus-mediated gene delivery into the scala media of the normal and deafened adult mouse ear. Gene Ther. 2011; 18:569–578. [PubMed: 21209625]
33. Kesser BW, Hashisaki GT, Fletcher K, Eppard H, Holt JR. An in vitro model system to study gene therapy in the human inner ear. Gene Ther. 2007; 14:1121–1131. [PubMed: 17568767]
34. Dilwali S, Landegger LD, Soares VY, Deschler DG, Stankovic KM. Secreted Factors from Human Vestibular Schwannomas Can Cause Cochlear Damage. Scientific reports. 2015; 5:18599. [PubMed: 26690506]
35. Liu L, Duff K. A technique for serial collection of cerebrospinal fluid from the cisterna magna in mouse. Journal of visualized experiments : JoVE. 2008
36. Sergeyenko Y, Lall K, Liberman MC, Kujawa SG. Age-related cochlear synaptopathy: an early-onset contributor to auditory functional decline. The Journal of neuroscience : the official journal of the Society for Neuroscience. 2013; 33:13686–13694. [PubMed: 23966690]

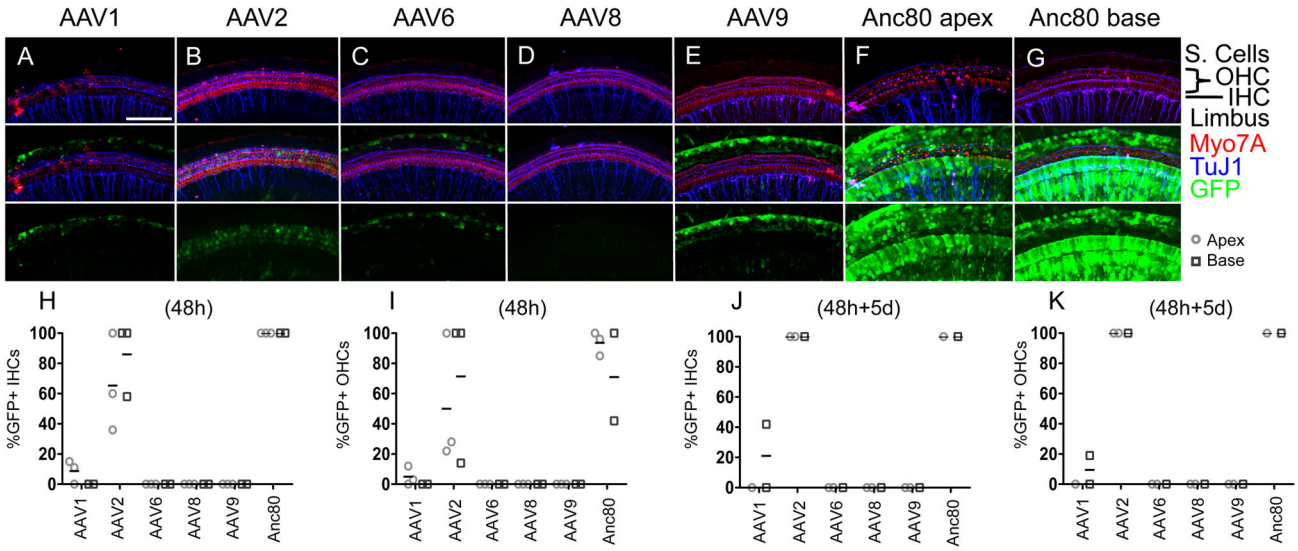

Figure 1. Transduction of organotypic explant of murine cochlea with natural AAV serotypes and Anc80L65

Representative confocal projections of an *in vitro* comparison of several AAV serotypes for eGFP transgene expression in cochlear explants of C57BL/6 mice. **A–G**: Expression at the cochlear base for all serotypes, and apex and base for Anc80L65 after incubation with 10^{10} genome containing (GC) particles for 48 hours. Scale bar = 100 μm. (Top: Myo7A+TuJ1, bottom: eGFP only, middle: overlay, S. Cells: Supporting Cells, OHC: Outer Hair Cell, IHC: Inner Hair Cell) **H–K**: Percentage of eGFP-positive hair cells per 100 μm after 48h or 48h+5 days of incubation. Mean indicated by horizontal bar. Each condition had minimally N=3 for the 48h, and N=2 for the 48h+5d unless otherwise noted.

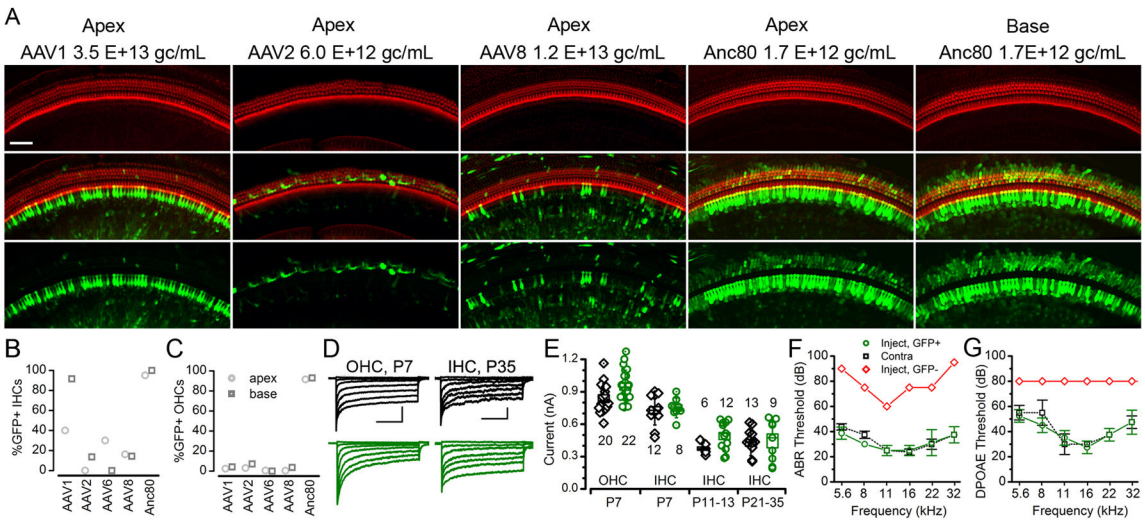

Figure 2. ***In vivo*** **cochlear transduction of natural AAV serotypes and Anc80L65**

(**A**) Confocal images of mouse organs of Corti, counterstained with Alexa546-phalloidin (red) and imaged for eGFP (green). A total of 5 (AAV1), 4 (AAV2), 2 (AAV8), 1 (AAV6), 3 (Anc80L65) C57BL/6 mice were injected with 1 μL of AAV stock solution in one ear at the titer indicated above each panel. Scale bar = 50 μm. Quantification of eGFP-positive IHCs (**B**) and OHC (**C**) in the base and apex of a representative AAV-eGFP injected cochlea for each vector. Quantification of eGFP-positive OHCs in the base and apex of AAV-eGFP injected cochleas. (**D**) Families of sensory transduction currents recorded at P7 (left) from eGFP-negative OHCs (black) and eGFP-positive OHCs (green). Hair bundles were deflected between −0.1 and 1 μm in 0.1 μm increments. Vertical scale bar indicates 200 pA; horizontal indicates 20 msec. Currents from eGFP-negative (black) and eGFP-positive (green) P35 IHCs are shown on the right. Vertical scale bar indicates 100 pA; horizontal indicates 20 msec. (**E**) Sensory transduction current amplitudes plotted for 103 IHCs and OHCs at the ages indicated at the bottom. Data from eGFP-negative (black) and eGFP-positive (green) are shown. The numbers of cells in each group are shown on the graph. All mice were injected at P1. (**F**) Mean ± standard deviation (SD). ABR thresholds plotted for four Anc80L65-injected ears (green) and four uninjected ears (black) together with data from one injected ear that had no eGFP fluorescence due to injection-related damage (red). (**G**) Mean ± SD. DPOAE thresholds are plotted for four Anc80L65-injected ears (green) and four uninjected ears (black) and one negative control ear with injection damage without eGFP fluorescence (red). Injection titers for data points in **B–G** are as in **A**.

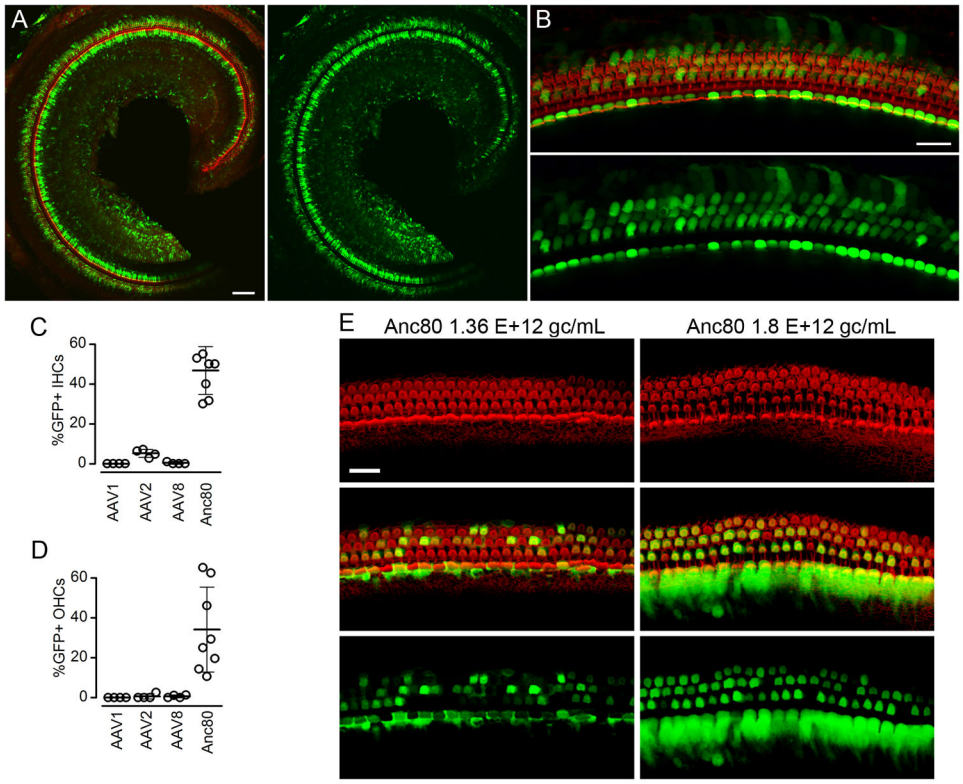

Figure 3. Extensive Inner and Outer Hair Cell transduction in murine cochleas with Anc80L65

Low- (**A**) and high (**B**) magnification image of the entire apical portion of a mouse cochlea injected at P1 with 1 μL of Anc80L65-eGFP at 1.70×10^{12} GC/mL. The cochlea was harvested at P10 and stained with Alexa546-phalloidin (red) and imaged for eGFP (green). Scale bar = 100 μm in (A), 20 μm in (**B**). (**C, D**) Quantitative comparison of inner and outer hair cell transduction efficiency at an equal dose for all serotypes following round window injection of P1-2 C57BL/6 mice. Mouse cochleas in (**C,D)** were injected with 1.36×10^{12} of AAV1, AAV2, AAV8, and Anc80L65 and harvested at 7–9 days for live-cell imaging and quantification by epifluorescence microscopy (n=8 per group unless otherwise noted). Error bars represent SD. (**E**) Dose-dependency of Anc80L65 hair cell transduction. Cochleas exposed to two different Anc80L65-eGFP titers (1.80×10^{12} versus 1.36×10^{12} GC) were fixed and stained with Alexa546-phalloidin (red) and imaged for eGFP (green). Scale bar = 20 μm.

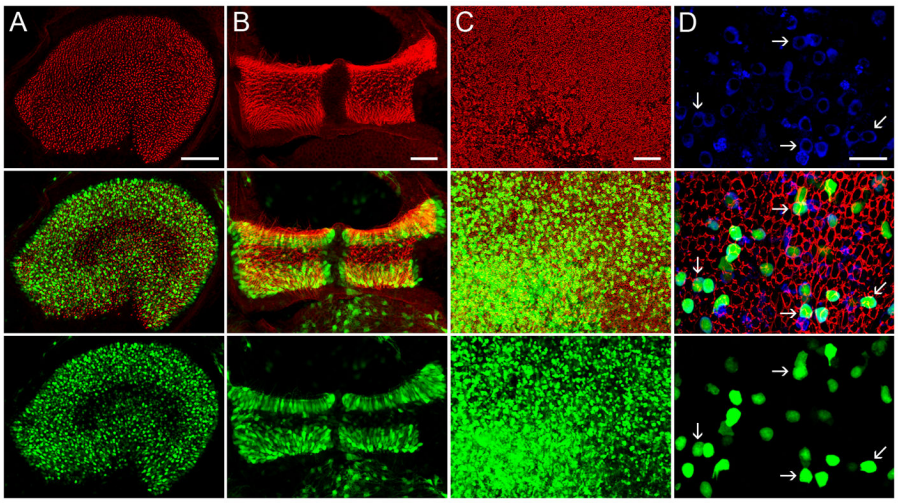

Figure 4. Anc80L65-eGFP transduction in vestibular sensory epithelia

(**A**) Mouse utricle from a P1 mouse injected with 1 μL Anc80L65-eGFP (1.7×10^{12} GC/mL). The tissue was harvested at P10 fixed and stained with Alexa546-phalloidin (red) and imaged for eGFP (green). Morphological assessment across multiple focal planes of eGFP-positive cells demonstrated transduction of stereotypical flask-shaped morphology of type I cells and the cylinder morphology of type II cells in every sample examined (not shown). Scale bar = 100 μm. (**B**) The crista of the posterior semicircular canal from the same mouse described for panel A. Scale bar = 50 μm. (**C**) The sensory epithelium of a human utricle. The tissue was exposed to 10^{10} GC Anc80L65.CMV.eGFP.WPRE for 24 hours, cultured for 10 days, fixed, stained with Alexa546-phalloidin (red) and imaged for eGFP fluorescence (green). Scale bar = 100 μm. (**D**) High-magnification view of a human epithelium in the utricle stained with Alexa546-phalloidin (red) and Myo7A (blue) and imaged for eGFP (green) transduced in identical conditions as in **C**. White arrows in the overlay panel indicate selected eGFP-positive/Myo7A-positive cells. Scale bar = 20 μm.